LBL-29919
Preprint

Lawrence Berkeley Laboratory
UNIVERSITY OF CALIFORNIA

Accelerator & Fusion Research Division

Submitted to Nuclear Instruments & Methods in Physics Research A

Performance of Electromagnet and Permanent Magnet Quadrupoles with Iron Poles

E.B. Blum and K. Halbach

October 1990

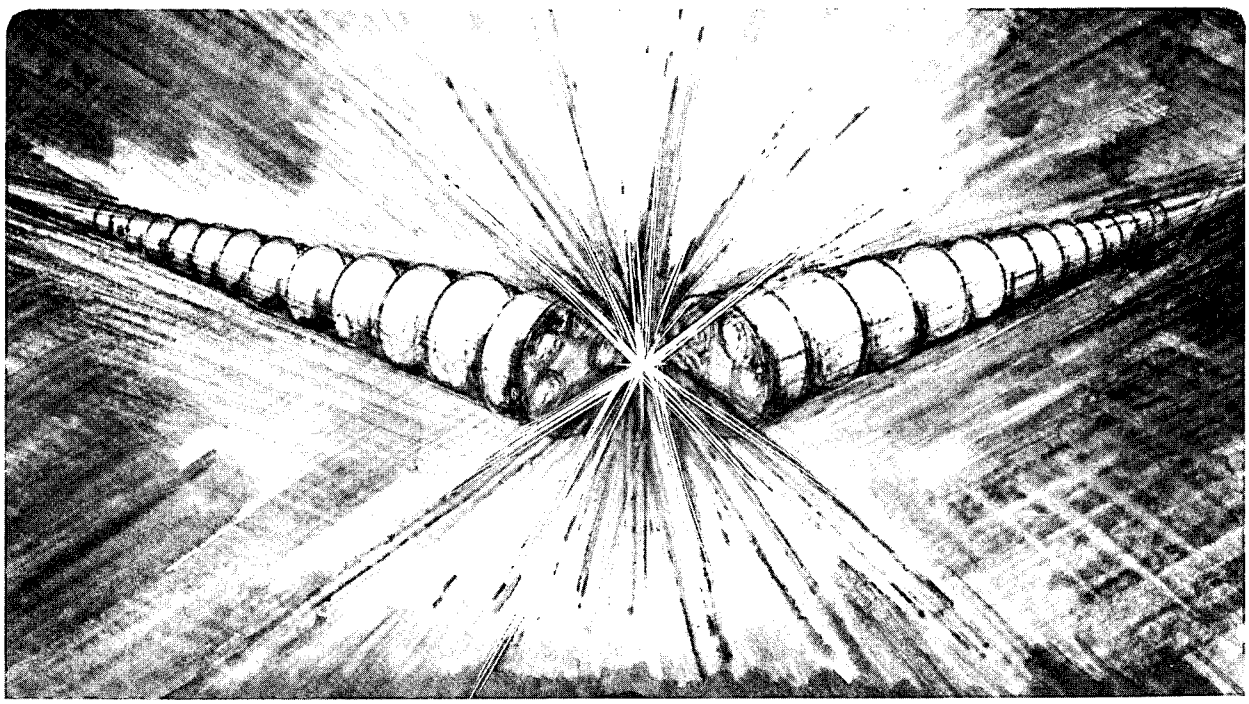

LOAN COPY
Circulates
For 4 weeks
EP Bldg. 50 Library
Lawrence Berkeley National Laboratory
LBL-29919
Copy 2

Prepared for the U.S. Department of Energy under Contract Number DE-AC03-76SF00098

DISCLAIMER

This document was prepared as an account of work sponsored by the United States Government. While this document is believed to contain correct information, neither the United States Government nor any agency thereof, nor the Regents of the University of California, nor any of their employees, makes any warranty, express or implied, or assumes any legal responsibility for the accuracy, completeness, or usefulness of any information, apparatus, product, or process disclosed, or represents that its use would not infringe privately owned rights. Reference herein to any specific commercial product, process, or service by its trade name, trademark, manufacturer, or otherwise, does not necessarily constitute or imply its endorsement, recommendation, or favoring by the United States Government or any agency thereof, or the Regents of the University of California. The views and opinions of authors expressed herein do not necessarily state or reflect those of the United States Government or any agency thereof or the Regents of the University of California.

LBL-29919

Performance of Electromagnet and Permanent Magnet Quadrupoles With Iron Poles*

E.B. Blum

Section of Biochemistry, Molecular, and Cell Biology
Cornell University, Ithaca, NY 14853

K. Halbach

Advanced Light Source
Accelerator and Fusion Research Division
Lawrence Berkeley Laboratory
1 Cyclotron Road
Berkeley, CA 94720

October 1990

Paper to be published in Nuclear Instruments & Methods in Physics Research A.

*This work was supported by the Director, Office of Energy Research, Office of Basic Energy Sciences, Materials Sciences Division of the U.S. Department of Energy, under Contract No. DE-AC03-76SF00098

PERFORMANCE OF ELECTROMAGNET AND PERMANENT MAGNET QUADRUPOLES WITH IRON POLES

E.B. BLUM
Section of Biochemistry, Molecular, and Cell Biology
Cornell University, Ithaca NY 14853

K. HALBACH
Lawrence Berkeley Laboratory, University of California, Berkeley, California 94720

Abstract

The largest field that can be obtained at the pole tip of an iron core quadrupole is limited by saturation in the iron and by its excitation by either the current density in the coil or the remanent field of the permenent magnet material. An analytical model is used to find the saturation limited performance of quadrupoles with either electromagnet or permanent magnet excitation. The results are presented in a form that can be used to evaluate proposed magnet designs but, more significantly, show that the strength of the excitation has less of an effect on the pole tip field than the size of the magnet needed to achieve it, and that saturation has more of an effect on the achievable field strength than excitation strength does.

1. Introduction

The largest usable field that can be obtained in an iron core magnet is limited by saturation in the iron and by its excitation either by the current density in the coil or the remanent field of the permanent magnet material. Although computer programs like POISSON[1] can be used to evaluate specific magnet designs in the presence of saturation, and can give extremely accurate results, they do not provide their users with any fundamental understanding of the behavior of the magnets. Computer methods may also be unacceptably slow on even the largest supercomputers when a large number of variables must be optimized in a design because an enormous number of runs may be needed to study all of the possible relevant configurations. Analytical approximations, however, can often predict the performance of a magnet to better than 10% accuracy, and more readily show the principles underlying its behavior.

1. POISSON is an improved version of TRIM [originally written by A.M. Winslow, J. Computer Phys. 1 (1967) 149] and was developed by J.R. Spoerl, R.F. Holsinger, and K. Halbach.

An analytical model is used to predict the maximum field that can be obtained at the pole tip of an iron core quadrupole with either electromagnet or permanent magnet excitation.[2] By symmetry, only the 45° segment of the magnet, shown schematically in fig. 1, is needed to understand the problem. Only two dimensional (2D) fields far from the ends of the magnet will be considered to avoid excessive mathematical complexities although the model can be extended to 3D. We assume that the iron has infinite permeability but account for saturation by restricting the maximum flux density in the pole to a value that is reasonable for the material used. The model can also be extended to incorporate finite but constant permeability below saturation. Similar models can be used to analyze higher order multipole magnets as well.

The results of the calculations will be presented in a general form that can be used to evaluate specific quadrupole designs. More importantly, they show that the strength of the excitation, whether remanent field in a permanent magnet or current density in an electromagnet, has less of an effect on the maximum pole tip field than on the size of the magnet needed to achieve it and that the saturation induction of the pole material has a much greater effect on the achievable pole tip field than the excitation strength does.

2. Electromagnet Quadrupoles

Dimensional analysis shows that the relationship between the pole tip field B_0, the saturation induction B_S, the aperture radius r_0, and the current density j in an electromagnet can be represented by a functional relationship between two dimensionless products. Of the many possible representations of this relationship, we will consider B_0/B_S as a function of $\mu_0 j r_0/B_S$ to study the limits on quadrupole performance, and will later use that information to plot $B_0/\mu_0 j r_0$ as a function of $B_S/\mu_0 j r_0$ to see the strong effects of saturation on performance more clearly. Our model is based on the following considerations:

1. The pole tip field B_0 is determined trivially by the number of Ampere-turns in the magnet coil which is just the current density j multiplied by the area of the coil.

2. The largest achievable field is considered limited when the maximum field anywhere in the pole is $|\overline{B}|_{\mathbf{max}} = B_S$, the saturation induction of the material. How this is obtained is complicated and will be described in detail below.

3. Referring to the cross-sectional view of an electromagnetic quadrupole in fig. 1a, the average field $\overline{B}$ on some slice through the pole, such as the one labeled *45* in the drawing, is given by the flux through the slice divided by the distance to the centerline $D(x)$.

---

2. We will be considering pole tip fields rather than field gradients because we will be using a model that is independent of the size of the quadrupole. The gradient in any particular quadrupole can of course be obtained by dividing the pole tip field by the aperture radius.

4. The field lines in the coil region are assumed to be circular arcs of constant magnetic field. The flux in the pole is the sum of the flux that enters the pole through the boundary with the coil and the flux that enters through the pole face (segment *0 1* in the drawing) with a correction for the fact that the field lines are not exactly circular near the end of the pole face (point *1* in the drawing).

One could optimize the geometry of the magnet by curving the boundary between the pole and the coil but this is not practical either for the analysis or for construction.

In formulating our model we will first derive a formula for the average field on any slice through the pole *4 5*

$$\overline{B} = G_0(x, \mu_0 j, r_0, B_0, x_1, x_2, \alpha_1, \alpha_2), \tag{1}$$

with the meanings of x, x_1, and x_2, indicated in fig. 1a. The angle α_1 is determined by the quality of the magnetic field that is required in the aperture of the quadrupole, and as we shall see, the strength of the pole tip field B_0 that can be obtained depends strongly on the value of α_2. Using the dimensionless variables

$$P_1 = \frac{B_0}{B_S}, \tag{2a}$$

$$P_2 = \frac{\mu_0 j r_0}{B_S}, \tag{2b}$$

and

$$P_3 = \frac{P_2}{P_1} = \mu_0 j r_0 / B_0, \tag{2c}$$

we will then recast eqn. 1 in the dimensionless form

$$\frac{\overline{B}}{B_0} = G_1(x/r_0, P_3, x_1/r_0, x_2/r_0, \alpha_1, \alpha_2). \tag{3}$$

The quantity G_1 will have a maximum at some x; we next associate that maximum value of G_1 with the saturation induction:

$$\frac{|\overline{B}|_{\max}}{B_0} = \frac{B_S}{B_0} = \frac{1}{P_1} = G_2(P_3, x_1/r_0, x_2/r_0, \alpha_1, \alpha_2). \tag{4}$$

We can therefore find the relative pole-tip field P_1 for any value of P_3, and from these obtain the relative excitation P_2 needed to produce it.

Now that we have outlined the logic behind our model, we will present its formulation in detail. The current I required to produce B_0 is given by the expression

$$\mu_0 I = \tfrac{1}{2}\mu_0 j \alpha_2 ({x_2}^2 - {x_1}^2) = \tfrac{1}{2} B_0 r_0. \tag{5}$$

Considering j given, eqn. 5 determines x_2. The magnetic field on any circular arc in the coil region , such as *3 4*, is assumed to be constant and is given by

$$B(x) = \frac{B_0 r_0}{2\alpha_2 x} - \frac{\mu_0 j}{2x}(x^2 - {x_1}^2). \tag{6}$$

The flux entering the iron through the coil between points *1* and *4* is therefore

$$F_1(x) = \int_{x_1}^{x} B(x)\,dx. \tag{7}$$

The flux $F(x)$ passing through the surface *4 5* within the pole is the sum of the flux F_0 that enters through the pole face *0 1* and the flux F_1 through the coil. The contribution from the pole face can be found from a conformal mapping of the quadrupole into dipole geometry[3]

$$F_0 = \tfrac{1}{2} B_0 r_0 E_1 \tag{8a}$$

where

$$E_1 = \frac{1}{\tan 2\alpha_1} + \frac{1}{\pi}(\alpha_1 + \alpha_2). \tag{8b}$$

The first term on the R.H.S. of eqn. 8b represents the flux that enters the pole face while the second term is a correction for the increased magnetic field on both sides of the edge of the pole. For a properly shimmed pole, the relationship between the tolerable relative field error $\Delta B/B$ within the aperture and α_1 is given to a good approximation by

$$1/\tan 2\alpha_1 = .75 - .14 \ln(|\Delta B/B|). \tag{9}$$

The average field in the iron along surface *4 5* is

$$\begin{aligned} \overline{B}(x) &= \frac{F(x)}{D(x)} = \frac{F_0 + F_1(x)}{D_1 + ax} \\ &= \frac{B_0 r_0 \left[E_1 + \ln(x/x_1)/\alpha_2\right] + \mu_0 j[{x_1}^2 \ln(x/x_1) - (x^2 - {x_1}^2)/2]}{2(D_1 + ax)} \end{aligned} \tag{10a}$$

where

$$a = \sin(\frac{\pi}{4} - \alpha_2) \tag{10b}$$

for $\alpha_2 > 0$. When $\alpha_2 = 0$,

$$\overline{B}(x) = \frac{B_0 r_0 (E_1 + x/y_0) - \mu_0 j x^2}{2(D_0 + x/\sqrt{2})}, \tag{10c}$$

where x in this case is measured from the point directly beneath point *1* in fig. 1a; this is easier to derive directly rather than by taking the limit of eqn. 10a.

What do these complicated expressions tell us about the behavior of the magnetic field in the iron? We see from the derivatives of eqns. 10a and 10c, that if $\overline{B}(x)$ has an extremum, it

3. K. Halbach, "Insertion Device Design", L.B.L. Internal Publication V-8811-1.1-16 (Mar. 1989).

must be a maximum. This means that at most one maximum can be found. In other words, the magnetic field will be largest at one location in the pole and will be less everywhere else. Obviously, the maximum field in the pole must be found at either x_1, x_2, or somewhere in between. From the values of $\overline{B}'(x)$ at the endpoints, x_1 and x_2, we find that the maximum is found either in the middle of the pole or at x_1, when $\alpha_2 < 45°$ but is found at x_2 when $\alpha_2 = 45°$.

To find the maximum usable field, we now follow the procedure described above and rewrite eqns. 10a and 10c in dimensionless forms:

$$\frac{\overline{B}(f)}{B_0} = \frac{E_1 + \ln(f/f_1)/\alpha_2 + P_3(f)\left[{f_1}^2 \ln(f/f_1) - \frac{1}{2}(f^2 - {f_1}^2)\right]}{2(d_1 + af)}, \tag{11a}$$

for $\alpha_2 \neq 0$, and

$$\frac{\overline{B}(f)}{B_0} = \frac{E_1 + f/g - P_3(f)f^2}{2(d_0 + f/\sqrt{2})}, \tag{11b}$$

for $\alpha_2 = 0$, where

$$f = \frac{x}{r_0}, \tag{11c}$$

$$f_1 = \frac{x_1}{r_0}, \tag{11d}$$

$$g = \frac{y_0}{r_0}, \tag{11e}$$

$$d_0 = \frac{D_0}{r_0}, \tag{11f}$$

and

$$d_1 = \frac{D_1}{r_0}. \tag{11g}$$

We then use eqn. 4 to predict the maximum usable pole tip field in the quadrupole from the maximum value of eqn. 11a or 11b.This can be obtained analytically from eqn. 11b when $\alpha_2 = 0$, but a numerical solution of eqn. 10a is required when $\alpha_2 > 0$. Finally, the required extent of the coil, x_2 can be found from eqn. 5.

Figs. 2 and 3 show plots of $P_1 = B_{0,\mathbf{max}}/B_S$ vs. $P_2 = \mu_0 j r_0/B_S$ for $\alpha_1 = 15.11°$ (which corresponds to an achievable field quality of 10^{-3} within a circle of radius r_0 centered about the origin), and a range of values of α_2. Lines corresponding to a measure of the quadrupole size

$$\frac{r_2}{r_0} = \frac{x_2 + x_a}{r_0} \tag{12}$$

are also shown. The two sets of curves can be used to predict the maximum pole tip field that can be produced in a quadrupole for given values of B_S, r_0, j, and α_2, and also predict the necessary coil length. An alternate horizontal axis is shown as well for the specific case where $j = 2$ kA/cm^2 (a generous limit for the maximum current density in a water cooled

copper coil) and $B_S = 1.8\,\mathrm{T}$ (approximately the saturation induction in soft iron). From this, one can estimate the maximum pole tip field that can be reached in a water cooled, iron core, electromagnetic quadrupole with a given bore radius.

Examining the graphs, it seems surprising that as P_2 goes to zero, P_1 approaches an asymptotic value that is *not* zero! This is possible within the framework of this theory because x_2 goes to infinity as P_2 goes to zero (see eqn. 2). If one puts a limitation on the size of the magnet, P_1 will be zero when $P_2 = 0$.

The asymptotic value of P_1 reached as P_2 goes to zero is plotted as a function of α_2 in fig. 4. This graph also shows that the optimal choice of α_2 is in the range from 5° to 10° for small values of P_2. Figs. 2 and 3 show however, that the best choice has $\alpha_2 = 0°$ when P_2 is large.

Figs. 2 and 3 show that for a given value of r_0, B_0/B_S increases slowly with increasing current density. Clearly, saturation in the iron is a stronger limit on magnet performance than current density. To emphasize the effect of saturation we have replotted the data from fig. 2 to show $B_0/\mu_0 j r_0$ as a function of $B_S/\mu_0 j r_0$ in fig. 5. The graph shows that for given r_0, j, and α_2, the achievable pole tip field B_0 increases nearly linearly with the saturation induction B_S. The insert in the figure shows a graph of B_0 vs B_S for the specific case with $r_0 = 2.54\,\mathrm{cm}$, $j = 2\,\mathrm{kA/cm^2}$, and $\alpha_2 = 15°$. Increasing B_S from 1.8 T to 2.5 T will increase B_0 for this design from 1.1 T to 1.5 T.

POISSON simulations were used to test the ability of the model to predict the largest poletip field that can be obtained before the iron saturates. POISSON results with and without saturation for a quadrupole design with $r_0 = 3.5\,\mathrm{cm}$, B_S from 1.8 T, $j = 2\,\mathrm{kA/cm^2}$, $\alpha_1 = 15.11°$ and $\alpha_2 = 5°$ are plotted in fig. 6 as a function of the quadrupole size r_2. Saturation effects do not appreciably reduce the field until r_2 is larger than the optimum value given by the model, $r_2 = 10.49\,\mathrm{cm}$. POISSON results at the optimum size are compared with the prediction of the model in Table 1. They agree to within 2%.

TABLE 1

COMPARISON OF MODEL AND POISSON RESULTS	
CALCULATION	B_0
POISSON (with saturation)	1.23 T
POISSON (without saturation)	1.24 T
model	1.25 T

3. Permanent Magnet Quadrupoles

Following the same approach taken in the last section, we now want to establish the relationship between the dimensionless variables

$$P_1 = \frac{B_0}{B_S}, \tag{13a}$$

$$P_2 = \frac{B_R}{B_S}, \tag{13b}$$

and

$$P_3 = \frac{P_1}{P_2} = \frac{B_0}{B_R}, \tag{13c}$$

for permanent magnet excited quadrupoles with iron poles,[4] where B_0 and B_S have the same meaning as before and B_R is the remanent field of the permanent magnet material. It is interesting to note that, contrary to the electromagnetic case, these expressions are independent of r_0, which means that the strength of a permanent magnet quadrupole (or any other permanent magnet) is independent of the bore radius.

Our analysis applies to "current sheet equivalent materials"[5] (CSEM) such as samarium cobalt or neodymium iron boron, with

$$B_R \approx \mu_0 H_c \tag{14}$$

where H_c is the coercivity of the material; we assume implicitly that this relationship is exactly true and, consequently, that the differential permeabilty of the material is exactly unity. The analysis can be easily extended to constant but non-unity values of μ. It does not, however apply to materials like alnico with non-linear $B(H)$ curves which would, however, be so weak as to be of very little interest.

Fig. 1b shows a schematic view of a 45° segment of the cross section of a permanent magnet quadrupole with iron poles. In order to establish the maximum usable pole tip field we will only examine the portion of the pole up to the point at x_2 where the field entering the side of the pole starts to have the opposite polarity from the field entering the pole tip. The rest of the magnet must also be designed but, if done properly, will not have a flux density that is larger in magnitude than $|B|_{\max}$ in the part under consideration.

To achieve the largest possible field, we assume that the CSEM is arranged in the configuration shown in fig. 1b. The CSEM can also be arranged with the easy axis and two sides of the block aligned perpendicular to the x-axis, but the pole tip field will be smaller and, in the following analysis, all values of B_R must be multiplied by $\cos\alpha_2$.

---

4. K. Halbach, I.E.E.E Trans. Nucl. Sci. **NS-30** (1983) 3323.

5. K. Halbach, Nucl. Inst. and Meth. **169** (1980) 1.

Following the notation of the last section, the total flux through the pole is

$$F(x) = \tfrac{1}{2}B_0 r_0 \left[E_1 + \frac{1}{\alpha_2}\ln\left(\frac{x}{x_1}\right)\right] - B_R(x - x_1), \tag{15}$$

for $\alpha_2 \neq 0$. The location x_2 is determined by $dF/dx = 0$, giving

$$x_2 = \frac{B_0 r_0}{2\alpha_2 B_R} = \frac{r_0}{2\alpha_2}P_3. \tag{16}$$

It is clearly pointless to consider cases where $x_2 < x_1$; i.e. we are only interested in cases where

$$P_3 > \frac{2x_1\alpha_2}{r_0} = \frac{\alpha_2\sqrt{2\tan\alpha_1}}{\sin\alpha_2}. \tag{17}$$

Again, similarly to the last section, we obtain

$$\overline{B}(x) = \frac{B_0 r_0\,[E_1 + \ln(x/x_1)/\alpha_2] - 2B_R(x - x_1)}{2(D_1 + ax)}, \tag{18a}$$

where

$$a = \sin(\frac{\pi}{4} - \alpha_2), \tag{18b}$$

or in dimensionless form,

$$\frac{\overline{B}(f)}{B_0} = \frac{E_1 + \ln(f/f_1)/\alpha_2 - 2P_3(f - f_1)}{2(D_1 + af)}. \tag{18c}$$

The largest usable pole tip field is thus given by the expression

$$\frac{1}{P_1} = \left[\frac{E_1 + \ln(f/f_1)/\alpha_2 - 2P_2(f - f_1)}{2(D_1 + af)}\right]_{\max}, \tag{18d}$$

which can now be evaluated numerically.

When $\alpha_2 = 0$ we similarly have

$$\frac{1}{P_1} = \left[\frac{B_0 r_0 E_1 + (B_0 r_0/y_0 - 2B_R)x}{2(D_0 + x/\sqrt{2})}\right]_{\max}, \tag{19}$$

where x is measured from the point directly beneath point *1* in fig. 1b. The behavior of this function is very simple, and depends on whether P_2 is less than or greater than

$$P_0 = \frac{1}{\sqrt{2}}\left(\frac{D_0}{y_0 E_1} - 1\right). \tag{20a}$$

When $P_2 < P_0$,

$$P_1 = \sqrt{2}y_0 + 2y_0 P_2, \tag{20b}$$

and the maximum field is found at $x = 0$. When $P_2 > P_0$, P_1 has the constant value

$$P_1 = \frac{\sqrt{2}D_0}{E_1}, \tag{20c}$$

but the maximum field is found at $x = \infty$. For any finite sized quadrupole, the maximum pole tip field will always be less than the limit given by eqn. 20c.

Fig. 7 shows a plot of P_1 vs. P_2 for $\alpha_1 = 15.11°$ (corresponding to a field quality of 10^{-3}), for a range of values of α_2. The graph also shows the limiting value of P_3, given by eqn. 17 and several lines of constant r_2/r_0, given by eqn. 12. As explained above, these lines never reach, but are asymptotic to, the constant portion of the curve of P_1 vs. P_2 for $\alpha_2 = 0°$ for which $r_2 = \infty$. Because P_2 is already greater than 0.5 for the CSEM that is now available, we see from the graph that any additional increase in B_R will not lead to increased pole tip fields.

We also see from fig. 7 that, as in the electromagnetic case, P_1 approaches a non-zero value as P_2 goes to zero. This limit is exactly the same as the limit for the electromagnetic quadrupole, plotted in fig. 4, which should not be too surprising since the two quadrupoles should behave exactly the same in the limit of vanishing excitation.

4. Conclusions

We have described a model that can be used to predict the maximum pole tip field achievable in an iron core quadrupole before the iron saturates. By using dimensionless variables, we formulated the model in a form that can be readily used to evaluate specific designs and have presented a series of graphs showing the results for magnets with 0.1% field quality. We have seen that the results of the model are in excellent agreement with POISSON simulations.

Most significantly, we have seen two surprising effects of saturation. The results show that excitation strength in both permanent magnet and electromagnet quadrupoles has less of an effect on the maximum pole tip field than on the size of the magnet needed to achieve it; i.e. an optimally designed magnet with a low current density in the coils will obviously be larger than one with a high current density but will reach nearly the same pole tip field. Second, they show that the saturation induction of the pole material has a much greater effect on the achievable pole tip field than the excitation strength does. This suggests that any future development of high saturation induction materials may be as revolutionary to the design of quadrupoles (and higher multipoles) as the development of permanent magnet materials such as samarium cobalt and neodymium iron boron was to the design of wigglers and undulators.

5. Acknowledgements

The authors would like to thank Robert Siemann for his helpful comments on the text. This work was supported by the Director, Advanced Energy Systems, Basic Energy Sciences, Office of Energy Research, US DOE Contract No. DE-AC03-76SF00098.

FIGURE CAPTIONS

Fig. 1a. Cross-section through 45° segment of an electromagnet quadrupole.

Fig. 1b. Cross-section through 45° segment of a permanent quadrupole. The magnetization direction of the permanent magnet material is indicated by arrows.

Fig. 2. Calculation of electromagnet quadrupole performance with $\alpha_1 = 15.11°$. The dark black lines show $P_1 = B_0/B_S$ as a function of $P_2 = \mu_0 j r_0/B_S$ for fixed values of α_2. The lighter grey lines show the results for fixed values of r_2/r_0. The intersection of a dark line with a light line, therefore, completely specifies the quadrupole geometry. An alternate horizontal axis is shown for the specific cas where $j = 2kA/cm^2$ and $B_S = 1.8\,\mathrm{T}$.

Fig. 3. Expanded view of fig. 2 for $P_2 < 0.5$.

Fig. 4. Assymptotic value of P_1 as a function of α_2 reached as P_2 goes to zero.

Fig. 5. Data from fig. 2 replotted to show $B_0/\mu 0 j r_0$ as a function of $B_S/\mu 0 j r_0$ for fixed values of α_2. The insert is a graph of B_0 vs. B_S for the specific case where $r_0 = 2.54\,\mathrm{cm}$, $j = 2\,\mathrm{kA/cm^2}$, and $\alpha_2 = 15°$.

Fig. 6. POISSON simulations of the pole tip field in an electromagnet quadrupole with $r_0 = 3.5\,\mathrm{cm}$, B_S from $1.8\,\mathrm{T}$, $j = 2\,\mathrm{kA/cm^2}$, $\alpha_1 = 15.11°$ and $\alpha_2 = 5°$. Saturation was taken into account using the internal saturation table for iron in the program. The calculations without saturation were for infinitely permeable iron.

Fig. 7. Calculation of permanent magnet quadrupole performance with $\alpha_1 = 15.11°$. The dark black lines show $P_1 = B_0/B_S$ as a function of $P_2 = B_R/B_S$ for fixed values of α_2. The lighter grey lines show the results for fixed values of r_2/r_0. The broken line an the far right corresponds to the limiting value of $P_3 = B_R/B_S$, given by eqn. 17.

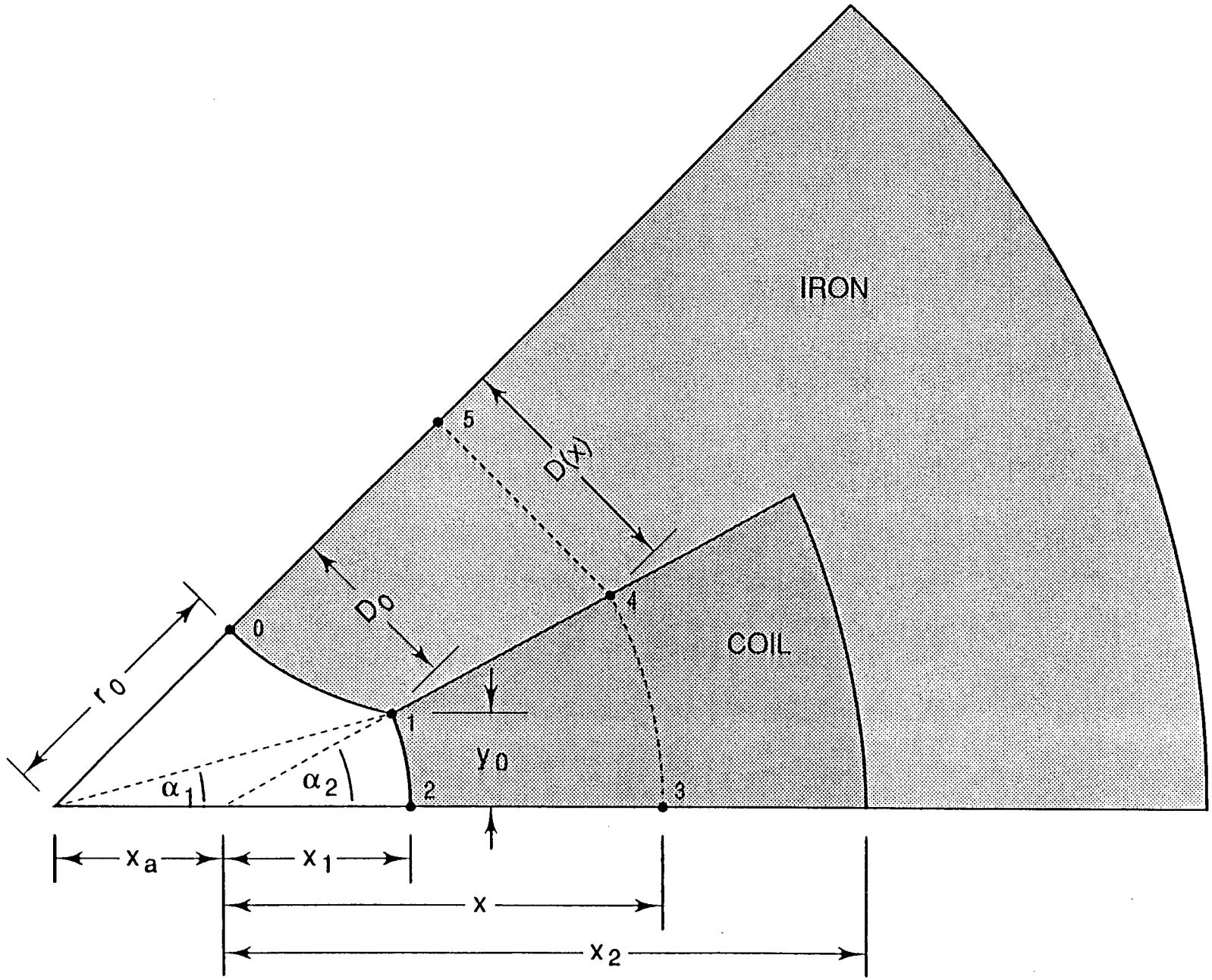

Figure 1a

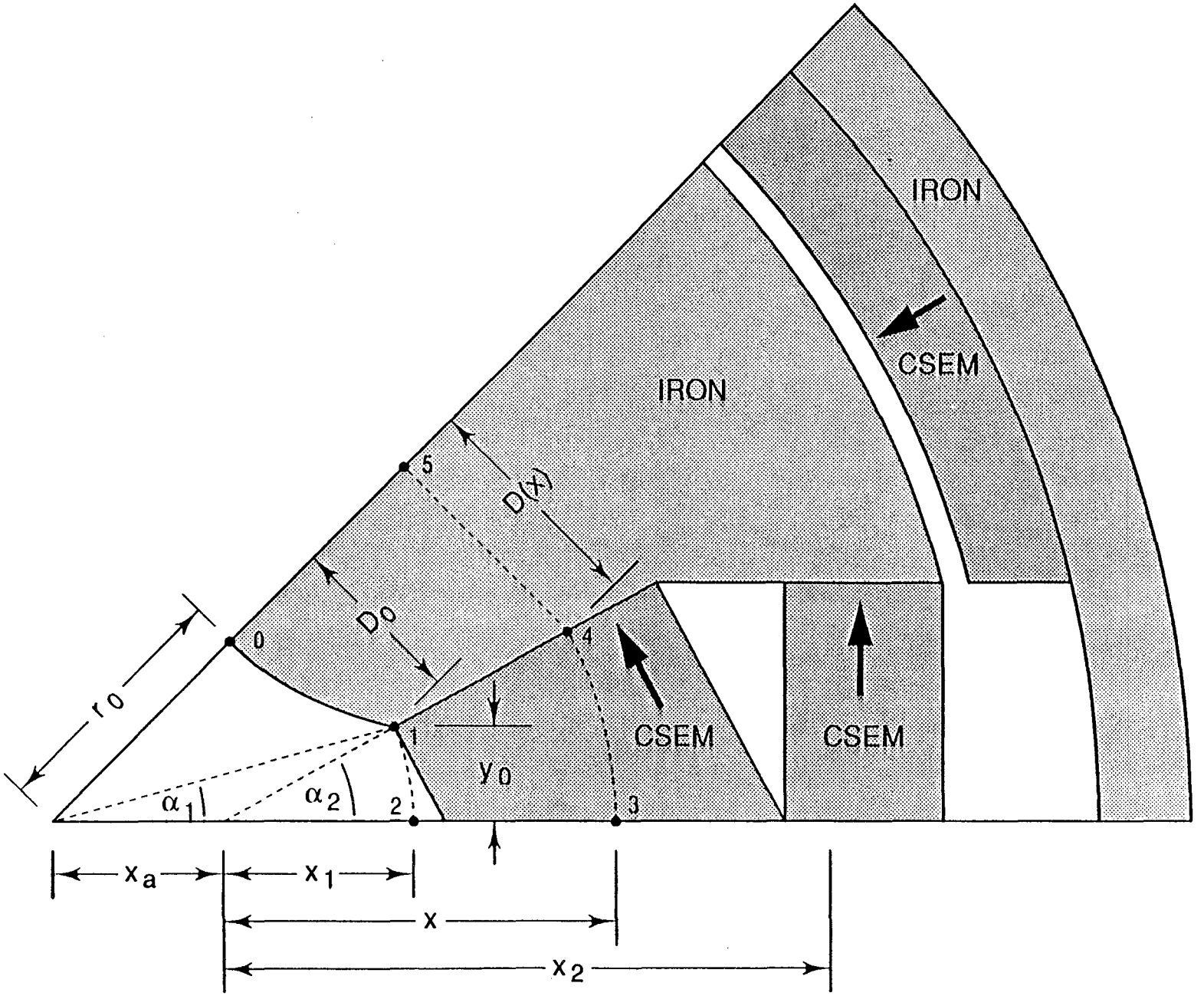

Figure 1b

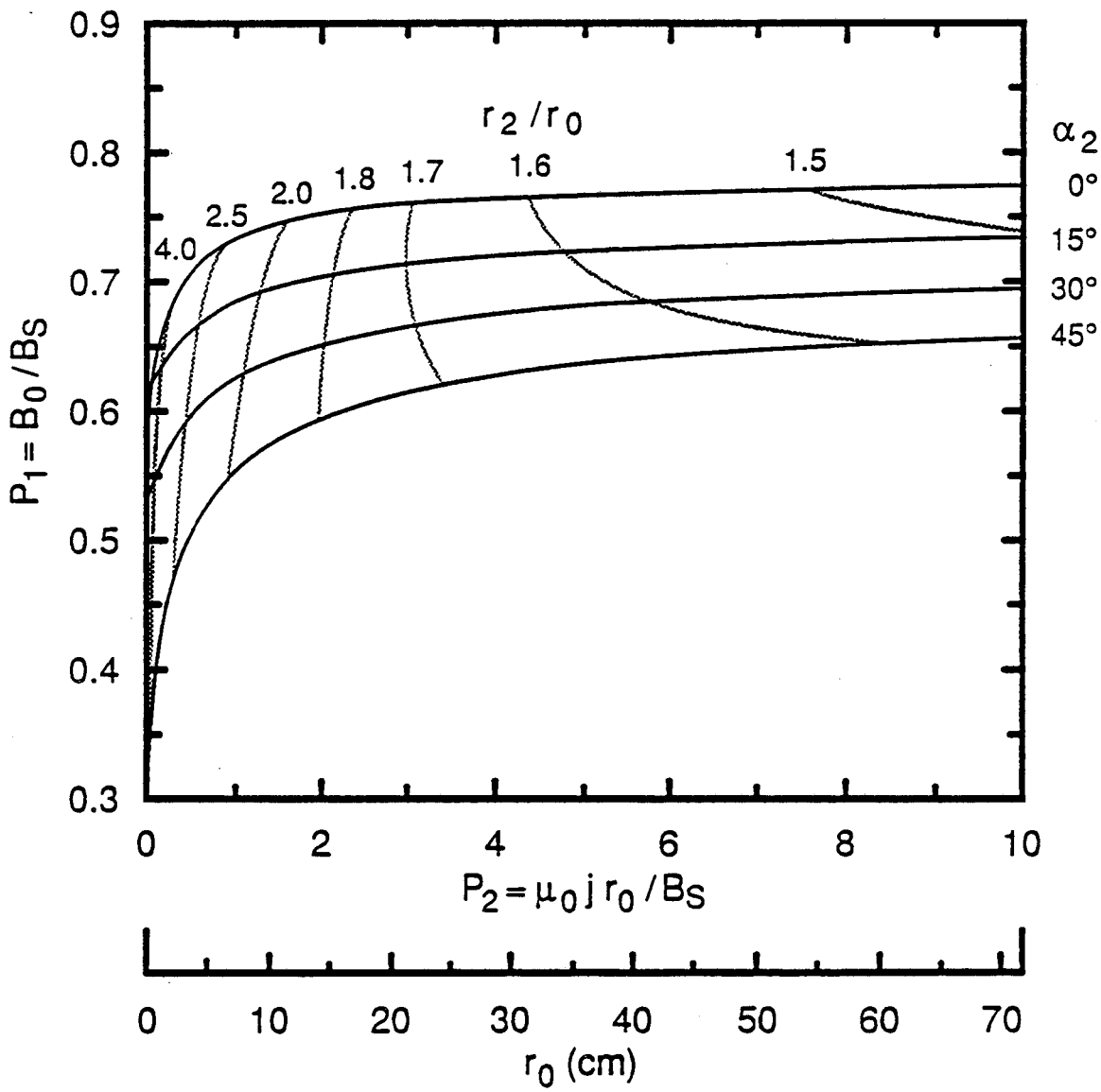
0.9
0.8
0.7
0.6
0.5
0.4
0.3
$P_1 = B_0/B_S$
r_2/r_0
4.0
2.5
2.0
1.8
1.7
1.6
1.5
α_2
0°
15°
30°
45°
0
2
4
6
8
10
$P_2 = \mu_0 j r_0/B_S$
0
10
20
30
40
50
60
70
r_0 (cm)

Figure 2

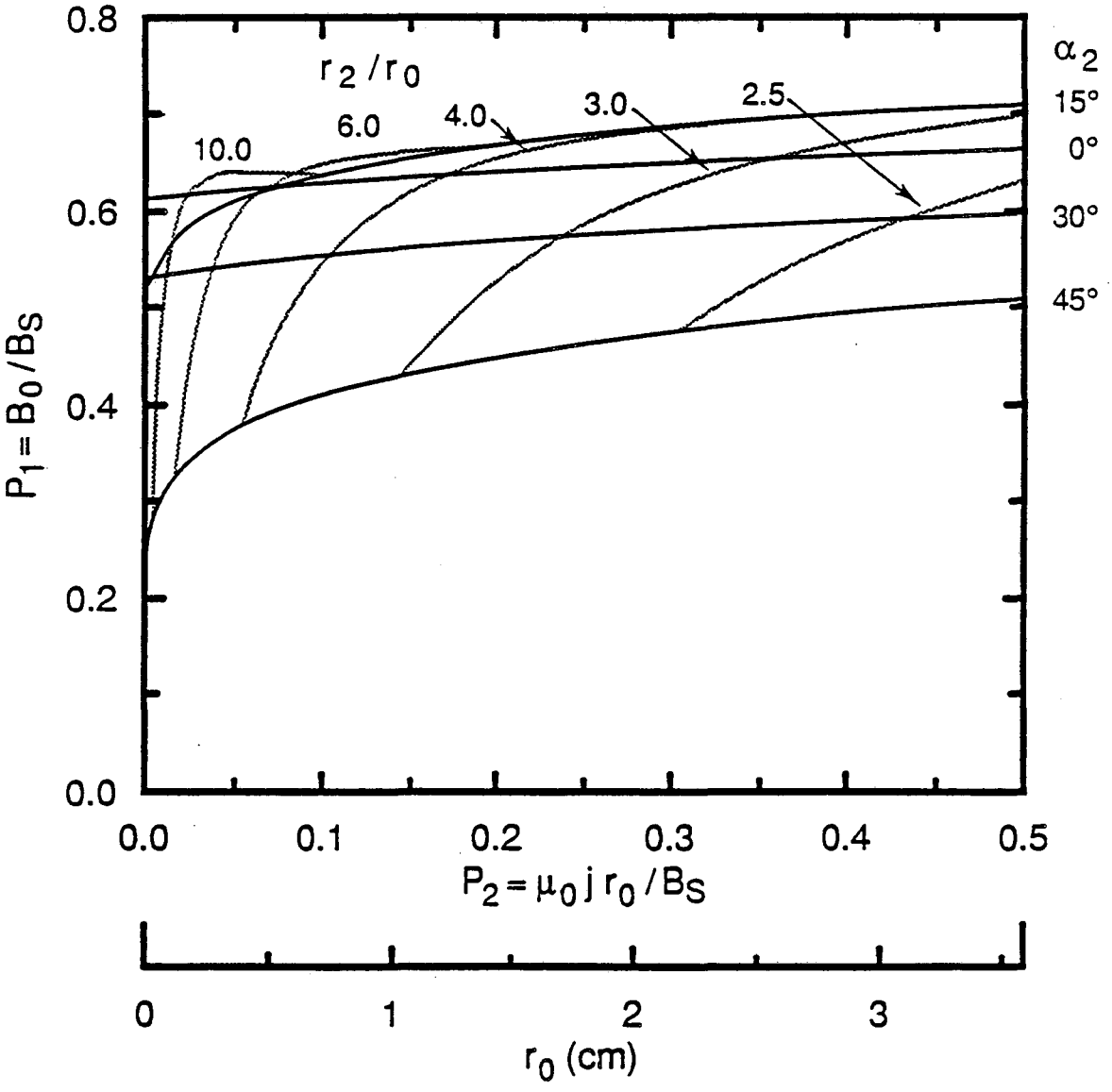
0.8
0.6
0.4
0.2
0.0
$P_1 = B_0/B_S$
r_2/r_0
10.0
6.0
4.0
3.0
2.5
α_2
15°
0°
30°
45°
0.0
0.1
0.2
0.3
0.4
0.5
$P_2 = \mu_0 j r_0/B_S$
0
1
2
3
r_0 (cm)

Figure 3

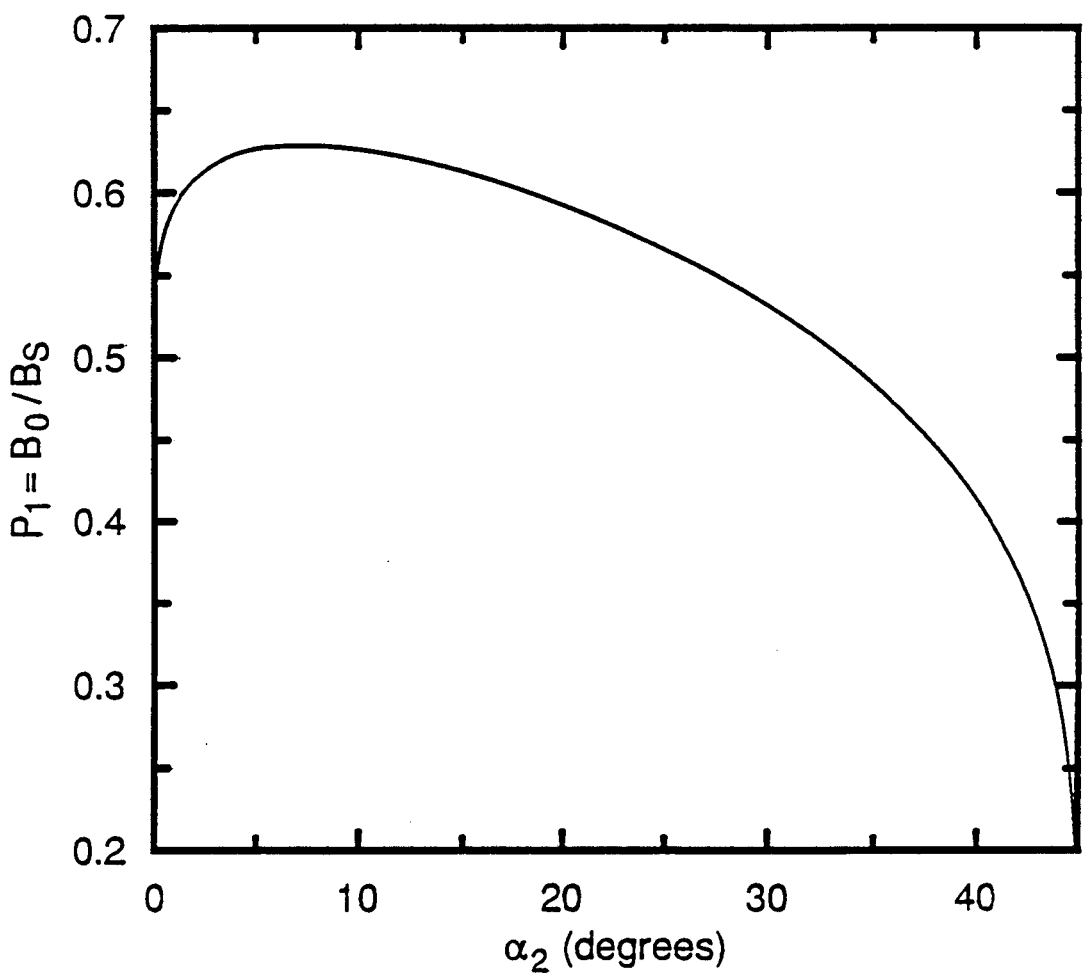

Figure 4

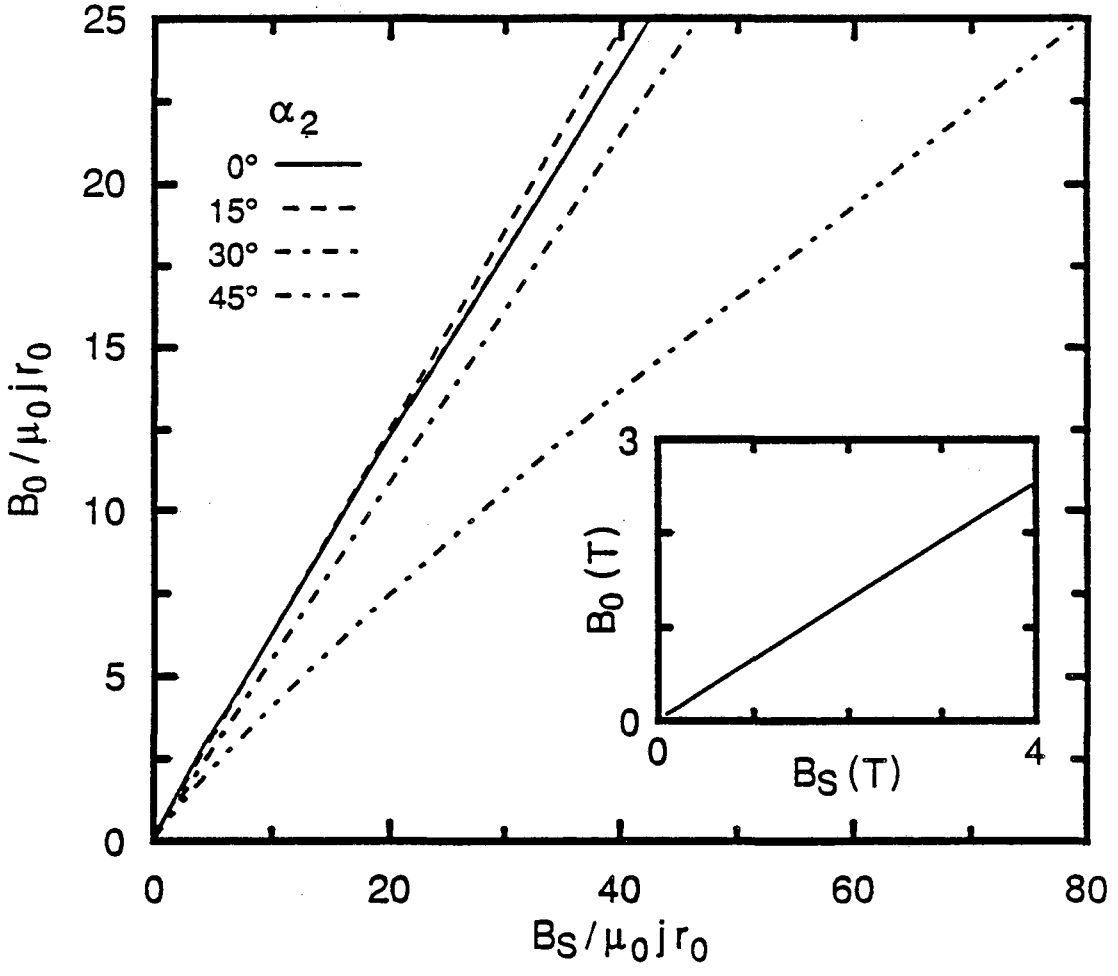
25
20
15
10
5
0
0
20
40
60
80
$B_0/\mu_0 j r_0$
$B_S/\mu_0 j r_0$
α_2
0°
15°
30°
45°
3
0
0
4
B_0 (T)
B_S (T)

Figure 5

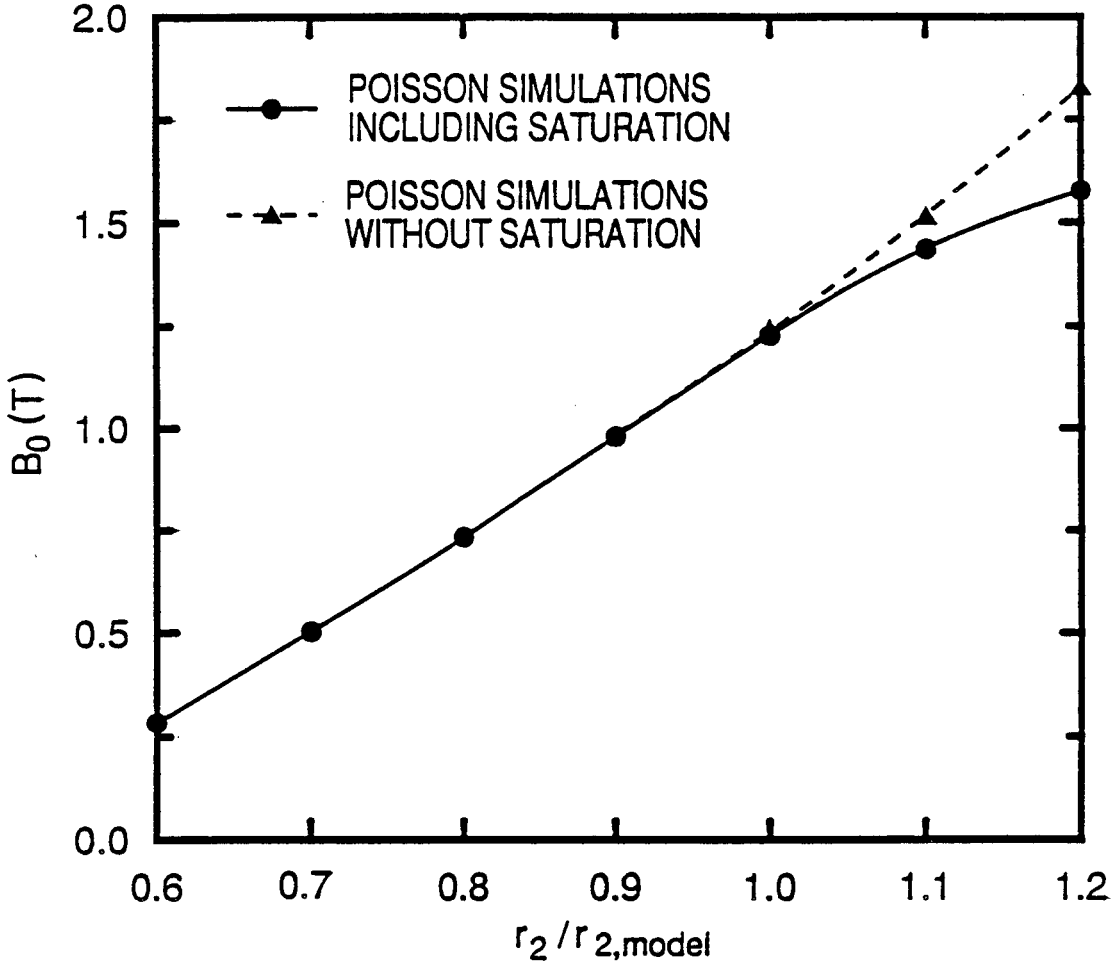
POISSON SIMULATIONS
INCLUDING SATURATION
POISSON SIMULATIONS
WITHOUT SATURATION
2.0
1.5
1.0
0.5
0.0
B_0 (T)
0.6
0.7
0.8
0.9
1.0
1.1
1.2
$r_2 / r_{2,model}$

Figure 6

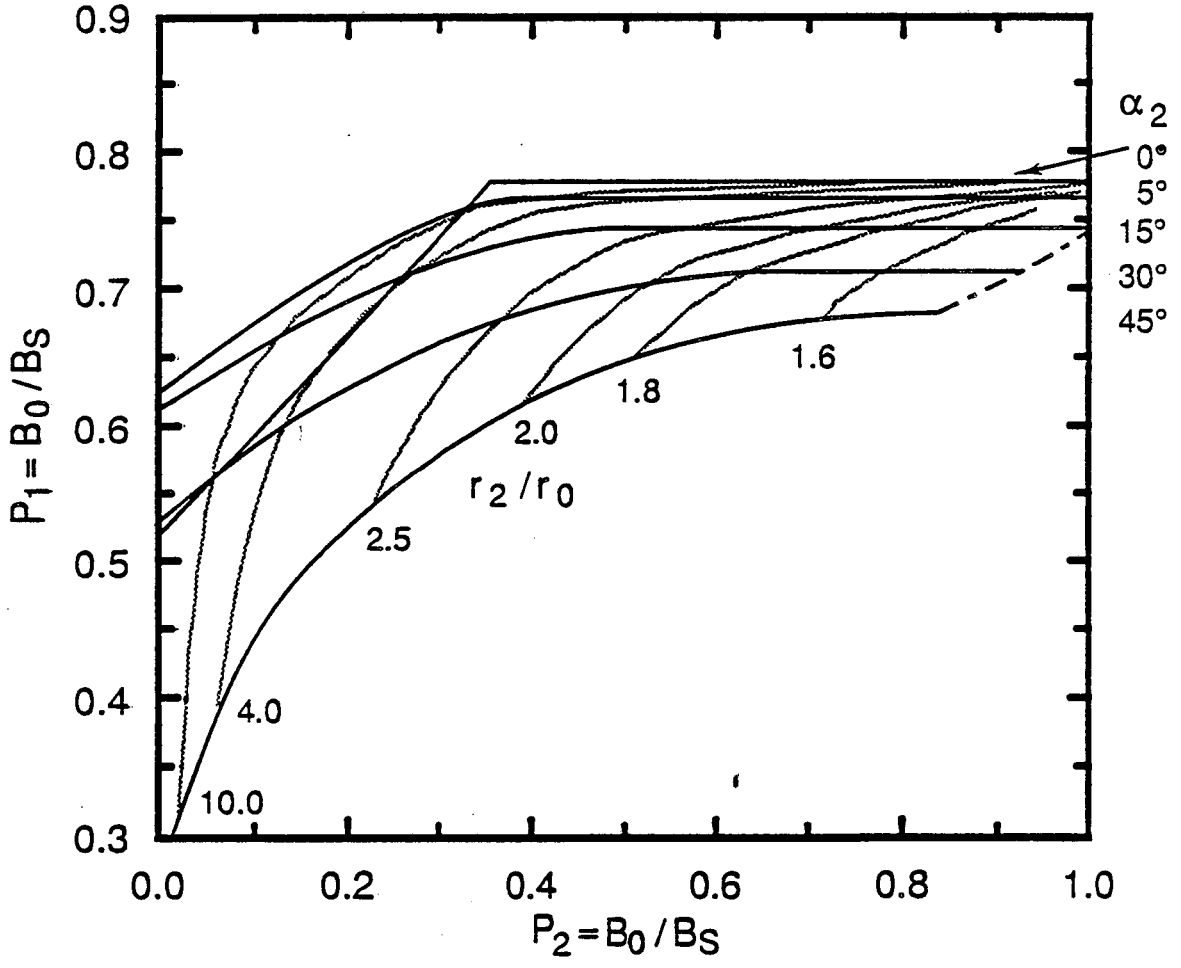
0.9
0.8
0.7
0.6
0.5
0.4
0.3
0.0
0.2
0.4
0.6
0.8
1.0
$P_1 = B_0/B_S$
$P_2 = B_0/B_S$
α_2
0°
5°
15°
30°
45°
1.6
1.8
2.0
2.5
4.0
10.0
r_2/r_0

Figure 7

LAWRENCE BERKELEY LABORATORY
UNIVERSITY OF CALIFORNIA
INFORMATION RESOURCES DEPARTMENT
BERKELEY, CALIFORNIA 94720

AAF341
LBL Libraries